Hindawi
Geofluids
Volume 2023, Article ID 5814341, 15 pages
https://doi.org/10.1155/2023/5814341

*Research Article*

# Weathering Processes and Mechanisms of Low-Grade Metamorphic Rock following Freeze-Thaw Processes

**Guopeng Wu**,[1,2] **Kai Cui**,[1,2] **Pei Wang**,[1] **and Wenwu Chen**[2]

[1]*School of Civil Engineering, Lanzhou University of Technology, Lanzhou 730050, China*
[2]*Key Laboratory of Mechanics on Disaster and Environment in Western China, Department of Geological Engineering, Lanzhou University, 222 Tianshui Road, Lanzhou 730000, China*

Correspondence should be addressed to Kai Cui; 65226683@qq.com

Received 18 April 2022; Revised 20 May 2022; Accepted 22 November 2022; Published 22 February 2023

Academic Editor: Di Feng



A remarkable risk in the field of rock engineering is the natural exposure of low-grade metamorphic rock to the freeze-thaw process. Examples of such materials are slate and phyllite, which are employed approximately mountainous permafrost zones. In order to study the weathering processes and mechanisms in low-grade metamorphic rock following freeze-thaw weathering processes, the freeze-thaw cycles were applied. Accordingly to this process, low-grade metamorphic rock partially or completely deteriorates, and mechanical properties, microstructure, and mineral content changes are commonly associated with freeze-thaw processes. This study shows that, following numerous freeze-thaw cycles processes, the quality, wave velocity, and compressive strength of rock reduce; calcite, mica, feldspar, and pyrite contents decrease; and clay minerals and gypsum content increase. Furthermore, the study also demonstrated that the changes in quality, wave velocity, and compressive strength caused by weathering of the rock followed the sequence slate > phyllite. However, the mineral contents of slate and phyllite alter in the same way. Because of this increase in volume and subsequent F-T cycles, new cracks form on the surfaces of pores due to outward pressure, and a lot of water is absorbed by clay minerals. The amount of water increases once again due to freezing as the temperature falls below zero degrees Celsius. This course duplicates with cyclic temperature changes and causes deterioration of low-grade metamorphic rock materials. By analysis of an examination of the damage variables based on wave velocity, it is possible to conclude that mineral changes during the freeze-thaw effect may make for the formation of voids and the deterioration of metamorphic rock. This research contributes to a better understanding of weathering processes and mechanisms of low-grade metamorphic rock following freeze-thaw weathering processes.

## 1. Introduction

Low-grade metamorphic rock, such as slate and phyllite, a thin rock found around mountainous permafrost regions, is weathered to the freeze-thaw process, and this represents a significant hazard in rock engineering. The rock can break down after F-T cycles and accumulates in valleys of mountainous permafrost regions, such as the Alps [1], the Himalayas [2], and the north-eastern edge of the Tibetan Plateau [3]. These large volumes of fragmentary material obstruct engineering construction and increase the risks of a wide range of geological hazards.

Temperature, moisture content, and rock type are the main factors causing rock damage [4–6]. The significance of temperature conditions, including minimum temperature and pace of decreasing, has been investigated in a number of studies [7], and moisture content has also been reported as a significant factor leading to rock failure following freeze-thaw cycles [8]. The mineral composition, the distribution of pore sizes, and the initial porosity of the rock are other characteristics that impact the chance of rock collapse [9–11].

Deterioration processes and mechanisms for pyrolith rock and sedimentary strata (granite, basalt, andesite, and sandstone, for instance) have been reported in mountainous permafrost regions [12–15]. To measure the effects of numerous cycles of freeze-thaw weathering, many physical and mechanical tests for sandstone have been developed, including the coefficient of compressibility, shear rate, specific resistance, uniaxial compressive strength, and triaxial compressive strength [16–20]. Similar to this, other physical and mechanical indices have been set up to describe the impact of freeze-thaw cycles on granites and andesites, including compressive strength, ultrasonic waved velocity, and hardness [21–24]. Bayram projected the uniaxial compressive strength of limestone after a certain number of freeze-thaw cycles [25]. Additionally, the weakening of rock in reaction to freezing temperatures may be determined by measuring the attenuation of ultrasonic wave velocity [26]. In summary, studies on the deterioration process and mechanism of rocks under different freeze-thaw environments are mainly focused on pyrolith rock and sedimentary rocks such as granites, sandstones, and shales, and there are few reports on low-level metamorphic rocks such as slates and phyllite under freeze-thaw effects.

However, overall, the number of studies on this topic in general is somewhat low, and even fewer systematic studies have been conducted on mineralogy and microscopic mechanisms of low-grade metamorphic rock following F-T weathering. Factors contributing to weakening of slate and phyllite through the action of water have not previously been identified. According to preliminary experiments, the mineral grains expand after absorbing water, which reduces the cementation between the mineral grains and improves the porosity, and the strength and failure modes of low-grade metamorphic rock are dependent on local variations in its structure [27–32]. Rocks that contain water lose some of their strength due to the weaker capillary force between grains.

In this study, macroscopic methods were applied to find the change law, and microscopic methods were used to detect microstructural changes in low-grade metamorphic rock, as it was experienced freeze-thaw cycles, to further investigate the failure mechanisms. Experiments were conducted after samples were encountered repeated freeze-thaw cycles, and its degree was ascertained using quality tests, wave velocity tests, uniaxial compression tests, and X-ray diffraction (XRD). After subjecting low-grade metamorphic rock to freeze-thaw weathering test, experiments were carried out. To clarify the weathering and behavioral mechanisms behind rock failures, the response of low-grade metamorphic rock to freeze-thaw weathering processes was evaluated. The results serve as a guide for assessing slope stability, estimating the likelihood of debris-flow disasters, and figuring out the safety measures required to maintain stability.

## 2. Materials and Methods

*2.1. Study Site.* To confirm weathering and behavioral mechanisms behind rock failures, the response of low-grade metamorphic rock to freeze-thaw weathering processes was evaluated. The results serve as a guide for assessing slope stability, estimating the likelihood of debris-flow disasters, and figuring out the safety measures required to maintain stability in the study area. During field investigations, we identified 281 mudslides occurring on one stratum of low-grade metamorphic rock within the Bailong basin (Figure 1). Furthermore, field investigations of landslide and mudslide gullies reveal that low-grade metamorphic rock within the slopes is easily crushed by gravity and other forces to create colluvial deposits. The surface of mudslide gullies contains low-grade metamorphic rock that weathers easily, adding mass to subsequent landslides. The subhumid climate, which varies greatly with elevation in study area, is favourable for freeze-thaw weathering processes.

According to examinations and investigation of mudslide occurrences, low-grade metamorphic rock is more likely to weather in areas where sliding surfaces and the accumulation of material in mudslide gullies are more common. For instance of Huoshao valley at Wudu (Figure 2), the source material reserve at the debris flow gully is $4,083.85 \times 10^4\,m^3$, and the source formed by falling from superficial rock mass is $2,829.4 \times 10^4\,m^3$, 69.2% of all source material. In addition, the investigation also finds that the source material reserve at debris flow gully falling from the metamorphic rocks of slate and phyllite slope is $1359.87 \times 10^4\,m^3$, 33.30% all source material. That means the weathering of metamorphic rock of slate and phyllite on the superficial slope under supergene processes is an important replenishment for source material of debris flow.

Evaporation and precipitation capacity from the Wudu regions show that precipitation capacity is greater than 20 mm from November to March, and the lowest surface temperature is -10°C. From November through March, the minimum monthly surface temperatures in Wudu are -5.1, -10.1, -10.5, -7.1, and -4.7°C. These results show that a freeze-thaw climate only lasts for a brief time in the area (Figure 3).

*2.2. Samples.* The samples were collected from 2 m below the typical slope at Huoshao valley in Wudu region. Polarized light microscopy was used to examine the structure of the samples (Figure 4). The slate has spherical and microscale spherical textures as well as microlaminar, lamellar, and dense massive structures, consisting mainly of sericite, quartz, lepidolite, and chlorite minerals (Figure 4(a)). The phyllite has an amphibolite texture and microlaminated, lamellar, and dense massive structure, consisting mainly of sericite, quartz, and smectite minerals.

The wave velocity of each sample was tested using an RSM-SY5 smart acoustic detector, and samples with similar wave velocities were selected. The experimental samples were extracted from folds in metamorphic rocks like slate and micrite that occurred naturally. The specimens are nonstandard cubic shapes with dimensions of 50 mm * 50 mm * their natural foliation. The samples were separated into ten groups, each with four pieces of metamorphic rock, then baked at 105°C for 48 hours to fulfil a consistent weight. After cooling, the samples were equilibrated at ambient temperature, and the dried samples were saturated with the proper vacuum venting apparatus. These samples were also weighed, and the key physical characteristics based on particle density were computed (Table 1).

*2.3. Methods.* To survey the process and mechanism of the low-grade metamorphic rock samples following freeze-thaw, a freeze-thaw test was applied. The two kinds of samples

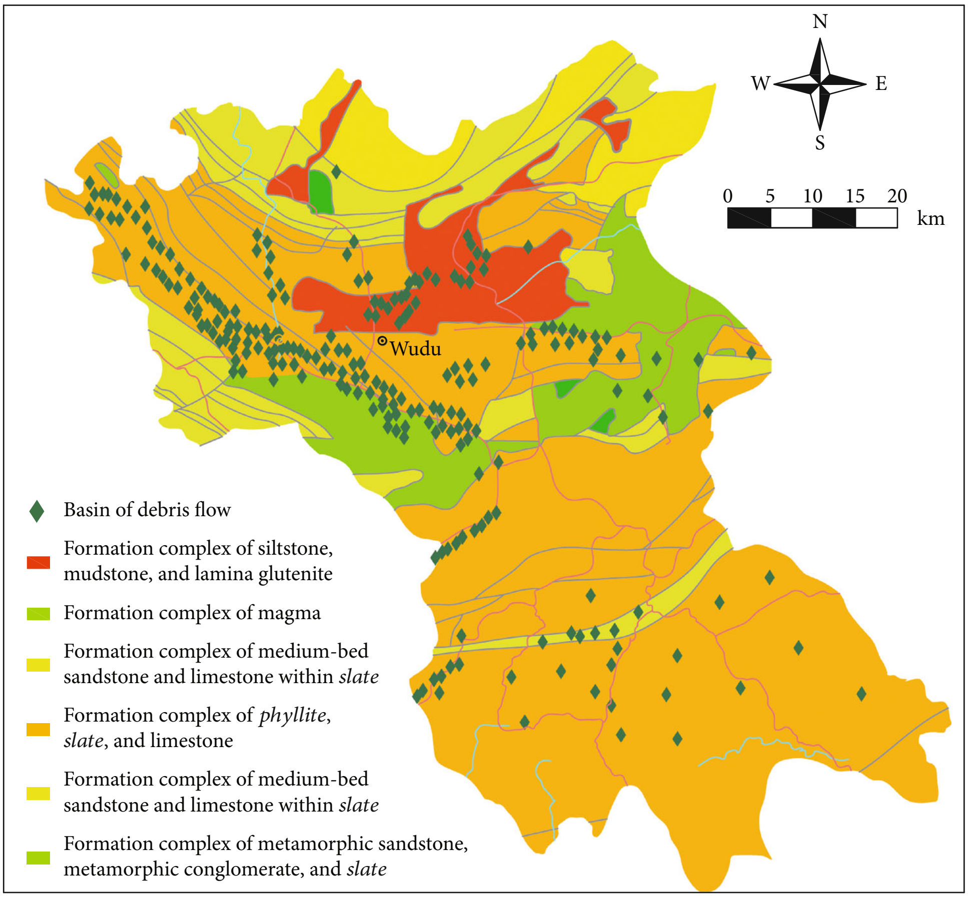


Figure 1: The sampling areas on a map of Wudu and representative debris flow gully.

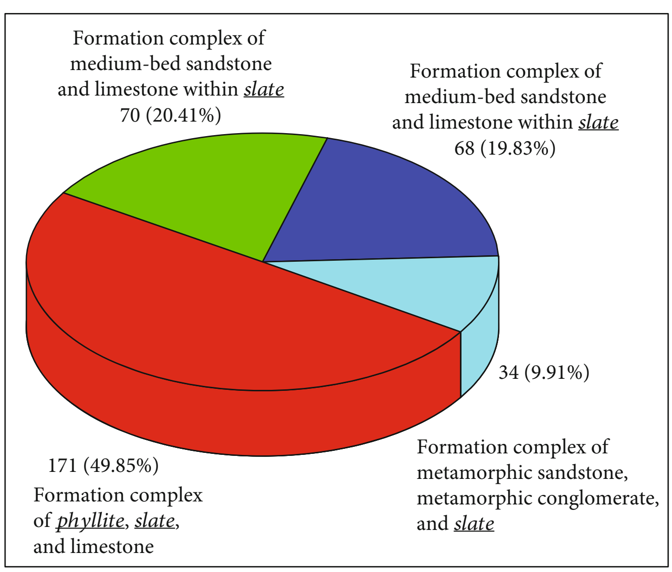


Figure 2: The mudslide on different formation.

were preserved and divided into five groups, each containing four metamorphic rocks of slate and phyllite, and subjected to 0, 5, 10, 20, and 30 F-T cycles, respectively. Quality, wave velocity, and uniaxial compression tests were performed in order to investigate the mechanisms causing changes in the samples' compressive intensity and velocity characteristics as a result of the F-T processes. In addition, X-ray diffraction (XRD) analysis and scanning electron microscopy (SEM)

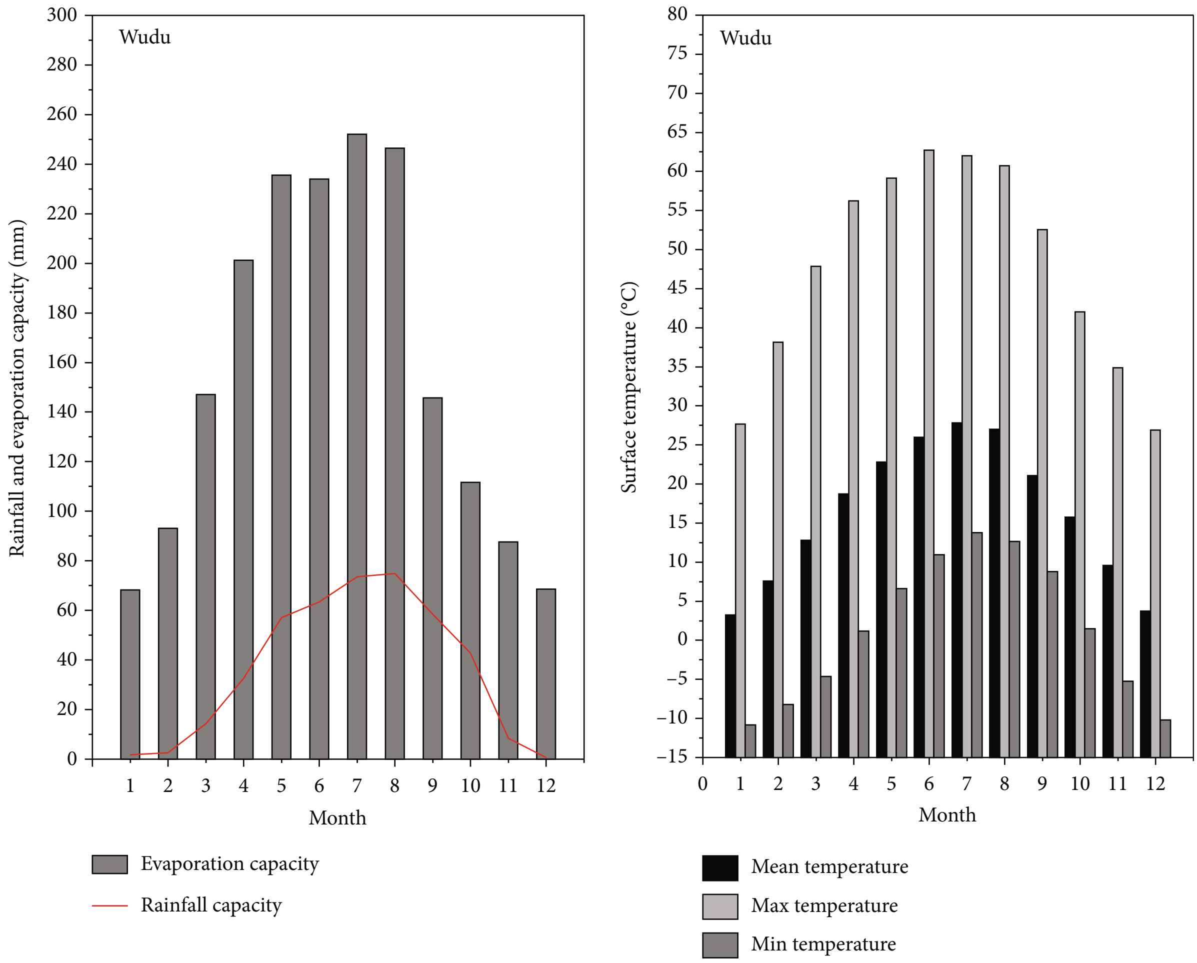


FIGURE 3: Monthly evaporation and precipitation capacity in Wudu.

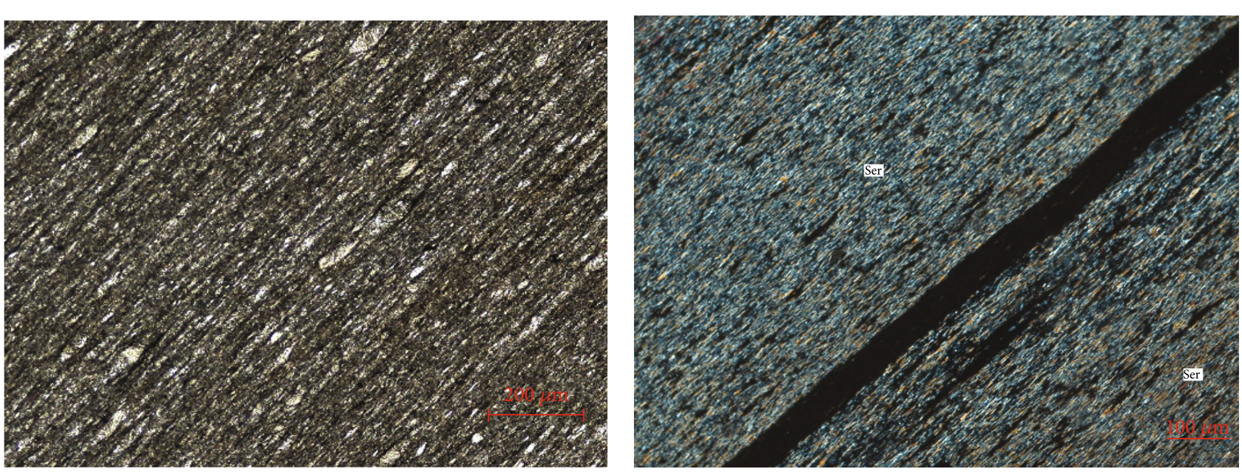


(a) Slate

(b) Phyllite

FIGURE 4: Mirror micrograph of two low-grade metamorphic rock samples.

analysis were performed on the samples to investigate the weathering mechanisms, and the variation in mineral composition and micromorphology in the samples encountered the freeze-thaw process.

The freeze-thaw experiments were conducted according to the Specification for Rock Testing in Water Conservancy and Hydropower Engineering (DL/T 5368-2007, China) and the Rock Testing Methods for Highway Engineering

Table 1: Primary index of two samples.

| Samples | Dry density Pd (g/cm$^3$) | Saturated density $P$ (g/cm$^3$) | Saturated moisture content ($\omega$ %$^{-1}$) | Porosity $\eta$ |
|---|---|---|---|---|
| S-0 | 2.47 | 2.60 | 1.61 | 2.31 |
| S-1 | 2.49 | 2.61 | 1.63 | 2.49 |
| S-2 | 2.48 | 2.60 | 1.62 | 2.32 |
| S-3 | 2.35 | 2.49 | 1.76 | 2.39 |
| S-4 | 2.55 | 2.59 | 1.56 | 2.32 |
| P-0 | 2.36 | 2.61 | 1.69 | 2.31 |
| P-1 | 2.46 | 2.68 | 1.61 | 2.31 |
| P-2 | 2.44 | 2.62 | 1.62 | 2.29 |
| P-3 | 2.34 | 2.55 | 1.61 | 2.31 |
| P-4 | 2.31 | 2.51 | 1.88 | 2.33 |

(JTG E41-2005, China) by repeatedly saturating low-grade metamorphic rock samples in distilled water at ambient temperature and then freezing them in a refrigerator at approximately -10°C. These experiments were performed for 12 hours.

## 3. Results

*3.1. Macromorphological Changes.* Surface cracks in the freeze-thaw weathering samples were parallel to the bedding plane orientation. The cracks in two low-grade metamorphic rock samples were all parallel to the layering. After 30 cycles, 13 surface fractures with maximum length and depth of 4.0 and 0.2 cm each were found on the slate samples. All of these fractures were parallel to the layering (Figure 5(a)). Only one surface fracture, parallel to the layers, with a maximum length and depth of 5.0 and 0.5 cm, respectively, was found in phyllite samples. (Figure 5(b)).

*3.2. Changes in Quality.* The requirements for test techniques of rock for highway engineering served as the foundation for the methodology created to evaluate the samples' quality. After the freeze-thaw, the quality of the sample was evaluated. The samples' quality barely changed as a result of freeze-thaw weathering. However, the samples that went through the freeze-thaw weathering process showed more obvious quality changes (Figure 6). The mass loss rate of low-grade metamorphic rocks was determined using the formula given in JTG E41-2005 part 5 (test methods of rock for highway engineering, 2005) as follows:

$$L = \frac{m_s - m_f}{m_s}, \tag{1}$$

where $L$ is the mass loss rate (%), $m_s$ is the quality of saturated specimens before freeze-thaw testing (g), and $m_f$ is the quality of saturated specimens after freeze-thaw testing.

The results showed mass loss rate increased quickly at first and decreased then with increasing number of weathering cycles in two low-grade metamorphic rocks (Figure 7). In contrast, mass loss rate increased before 5th freeze-thaw cycle and decreased after 20th freeze-thaw cycle in the following order: slate > phyllite.

*3.3. Changes in Wave Velocity.* An RSM-SY5 intelligent acoustic detector was used to analyze the wave velocity of the vertical aspects of the two low-grade metamorphic samples. Wave velocity decreased across the board in all experimental samples as the number of weathering cycles rose (Figure 7). The freeze-thaw series of phyllite samples differ from the slate samples, which underwent studies that showed a 21.44% decrease in wave velocity.

*3.4. Variation in Uniaxial Compression.* The findings demonstrated that the shift to uniaxial compression characteristics grew more significant as the number of cycles increased (Figure 8). The coefficient of freezing resistance of two low-grade metamorphic rocks was determined using the formula given in JTG E41-2005 part 5 (test methods of rock for highway engineering, 2005) as follows:

$$K_f = \frac{R_f}{R_s}, \tag{2}$$

where $K_f$ is the coefficient of freezing resistance, $R_f$ is the compressive strength of saturated specimens after freeze-thaw testing (MPa), and $R_s$ is the compressive strength of saturated specimens before freeze-thaw testing (MPa).

For slate, the coefficient of freezing resistance of the slate decreased quickly in the freeze-thaw series, from 1.0 to 0.792 (20.8%), by the 5th cycle. The proportion of coefficient of freezing resistance of the slate lost increased from 32.95% to 65.73% and, finally, to 58.79% at all stages of the freeze-thaw cycle. The strength of the slate sample dropped by 92.5% overall. By the fifth F-T cycle, the freezing resistance coefficient of phyllite has dropped from 1 to 0.942 (5.8%). The sample strength was reduced by 36.8%, while the proportion of overall strength lost fell from 7.22% to 9.73% to 19.9% at all stages of the freeze-thaw cycle, respectively.

*3.5. Features of Stress-Strain Curves.* Uniaxial compression studies conducted after experimental weathering identified significant similarities between the stress-strain curves of the two low-grade metamorphic rock sample groups. From loading and transformation until destruction, four separate phases were found. The following terms are stated in that order: yield, failure, elastic deformation, and compaction-deformation. The gradients of the stress-stain curves shifted downward for all of the slate samples, showing that the modulus of deformation dropped as the number of weathering cycles increased. With more weathering cycles, the compaction-deformation stage's duration also became longer, but the elastic and yield stages also reduced. Finally, when more weathering cycles occurred, the samples' yield strength and ultimate strength dropped (Figure 9).

The stress-strain curves of the phyllite and slate samples showed distinct differences after the freeze-thaw cycles. In every experiment, the modulus of deformation, yield strength, and ultimate strength was reduced by slate compared to phyllite. During freeze-thaw testing, the properties

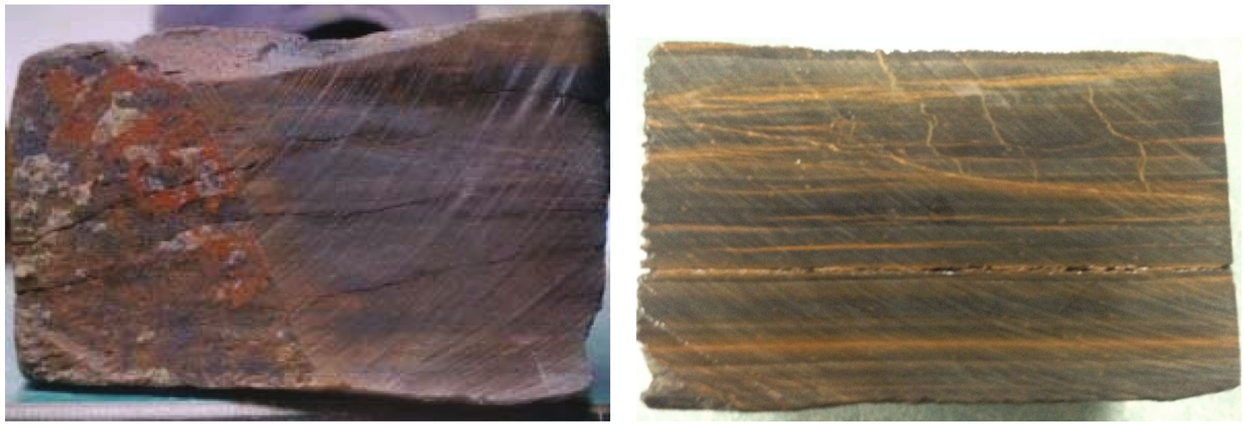


Figure 5: Variation of morphological at 30 F-T cycles of two low-grade metamorphic rocks.

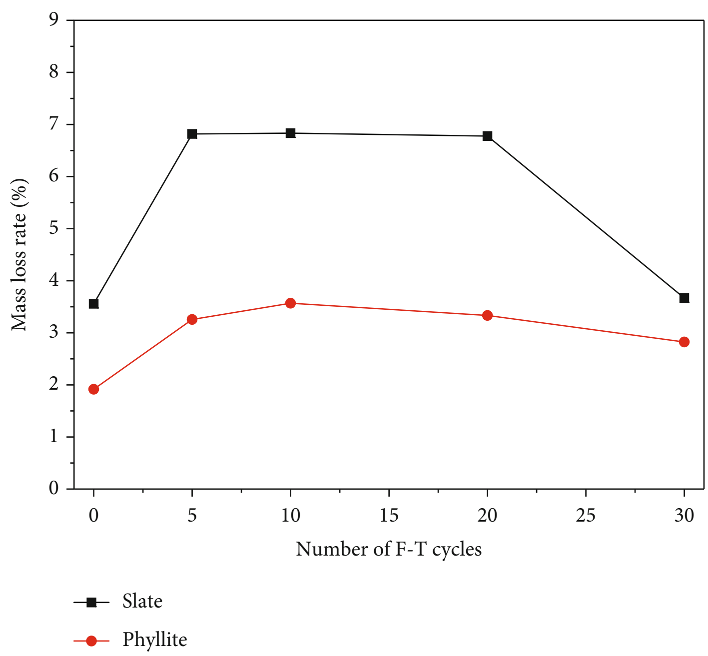


Figure 6: Relationships between mass loss rate and number of F-T cycles of two low-grade metamorphic rocks.

of slate's yield and failure phases were varied, and the samples also displayed various ductility traits. On the other hand, freeze-thaw experiments on phyllite samples failed to distinguish between yield and failure stages, but they did highlight particular stiffness traits.

*3.6. XRD Analysis.* XRD analysis was conducted on two low-grade metamorphic rock samples undergone F-T cycles to investigate changes in mineralogical composition. The 50 g air-dried samples collected from uniaxial compression test were passed through a 0.075 mm sieve, and different treatments (i.e., air-drying, heating, and glycolation) were applied to XRD tests. A Philips PW 3710 diffractometer was used for XRD analysis of the three slides. The diffraction patterns were determined using Cu–K$\alpha$ radiation with a Bragg angle ($2\theta$) range of 3–30°, running at a rate of 0.05°/s.

Figure 10 shows the distributions of minerals in two low-grade metamorphic rock samples subjected to different numbers of F-T cycles. Based on the XRD analyses, the two low-grade metamorphic rock samples were composed of minerals including quartz, mica, calcite, feldspar, pyrite, gypsum, and clay minerals. Figure 11 also indicates the relative contents of clay minerals and gypsum increased with increasing number of F-T cycles, while the relative contents of calcite, mica, feldspar, and pyrite decreased. In addition, Figure 10 also shows that the change law of the minerals in slate is similar to it in phyllite and that the number of different content of mineral is different. The content of clay and gypsum followed the sequence of slate > phyllite, but the content of mica, feldspar, calcite, and pyrite followed the sequence of slate < phyllite.

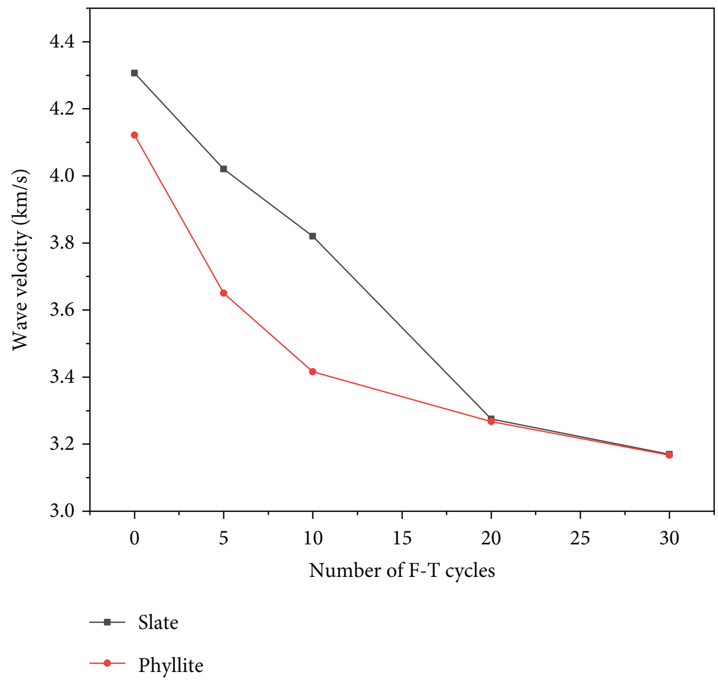


FIGURE 7: Wave velocity of two samples following freeze-thaw cycles.

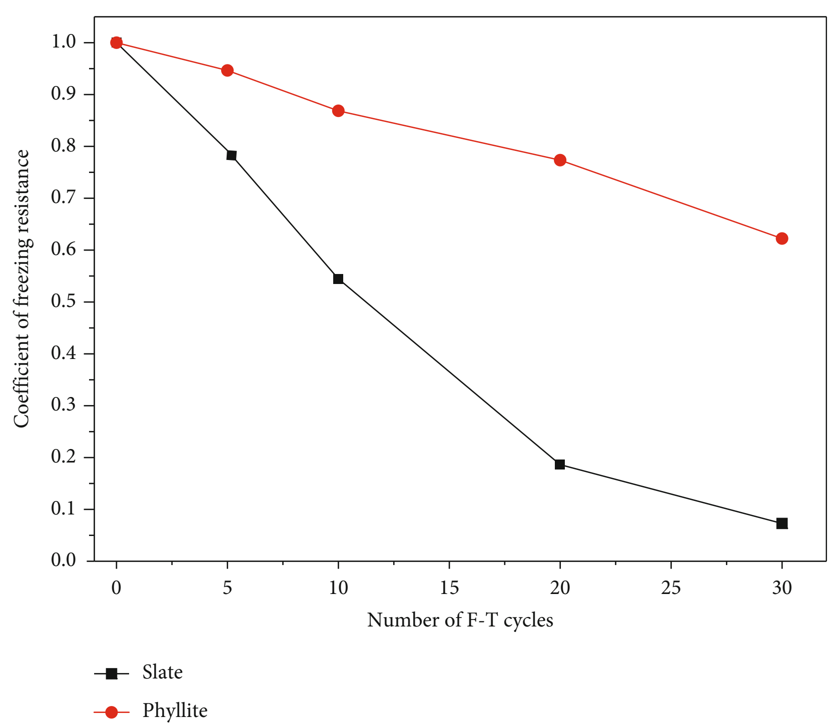


FIGURE 8: Relationships between coefficient of freezing resistance and number of F-T cycles of two low-grade metamorphic rocks.

*3.7. Microstructural Features.* SEM analysis was conducted on two low-grade metamorphic rock samples undergone F-T cycles to investigate changes in mineralogical composition.

The particle size of the specimen showed a pattern of increasing first, then keeping the same, and finally increasing again [33–37]. Specifically, from beginning to 5 times, the particle size of the specimen increased from 6-15 $\mu$m to 10-20 $\mu$m in slate and from 4-10 $\mu$m to 6-10 $\mu$m in phyllite. From 5 times to 10 times, the particle size remained unchanged, 10-20 $\mu$m in slate and 6-10 $\mu$m in phyllite. From 10 times to 20 times, the particle size changed again, from 6-15 $\mu$m to 10-20 $\mu$m in slate and from 4-10 $\mu$m to 6-10 $\mu$m in phyllite. At last, the particle size changed significantly to 20-25 $\mu$m in slate and 10-18 $\mu$m in phyllite. The

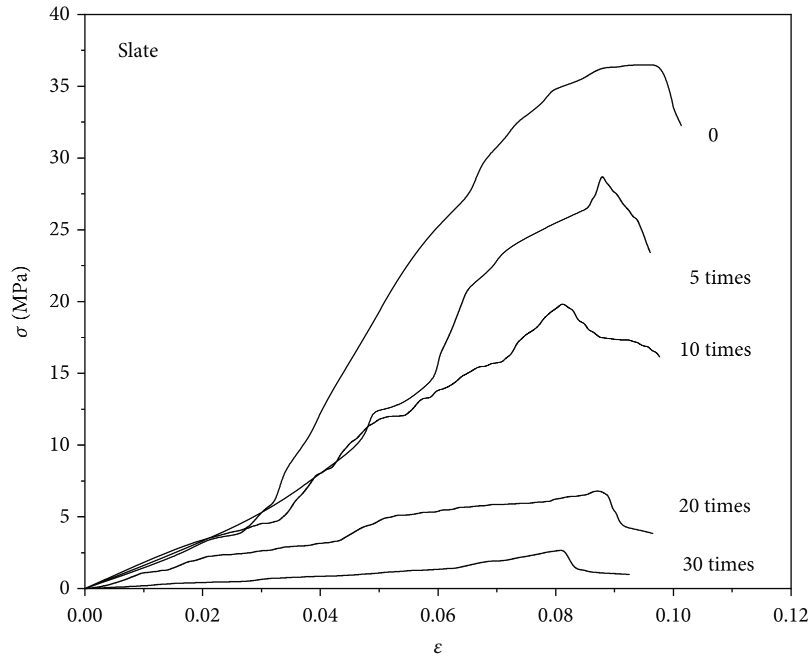


(a) Slate

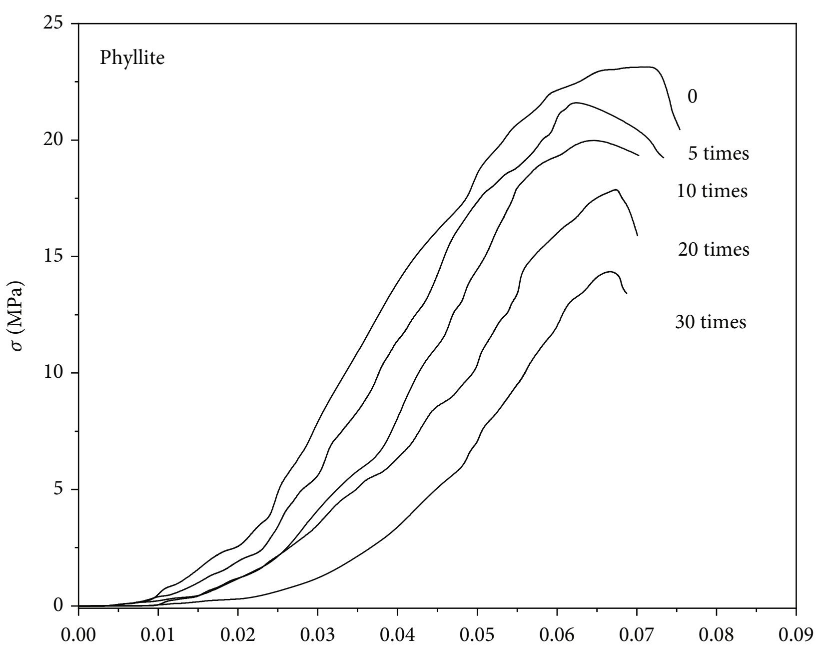


(b) Phyllite

Figure 9: Stress-strain curves for slate and phyllite samples.

specimens showed the following pattern: 0 and 5 times of maintenance showed "clearer local openings," and 10, 20, and 30 times of maintenance showed "loose openings." Additionally, the specimens showed a loose shape at 10, 20, and 30 times of maintenance. We also found that the parameters of adhesion, compactness, porosity (%), pore width ($\mu$m), etc., showed similar patterns to those of particle size, which are not repeated here, as detailed in Table 2.

## 4. Discuss

*4.1. Analysis of Results.* Low-grade metamorphic rocks produced by local metamorphism, such as slate and phyllite, frequently become exposed in places that are undergoing complicated deformation, including the current study sites. This regularly results in dangerous occurrences like mudslides and landslides. Slate and phyllite are examples of

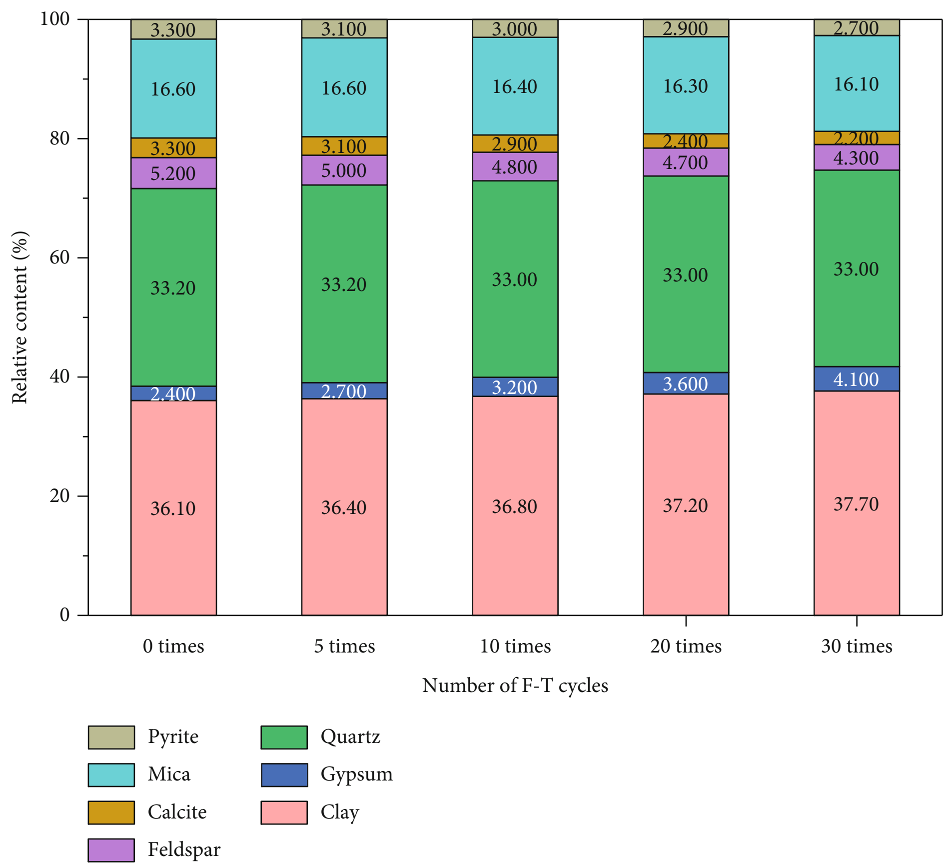


(a) Mineral content variation in slate

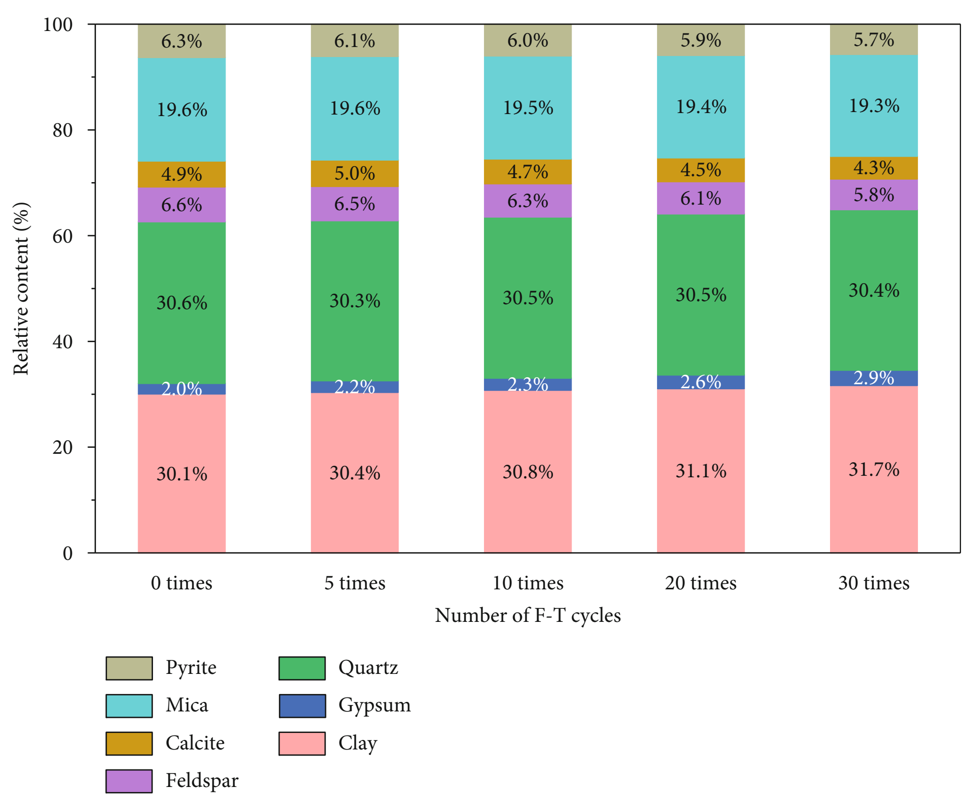


(b) Mineral content variation in phyllite

Figure 10: X-ray diffraction (XRD) scans of two low-grade metamorphic rocks with increasing number of F-T cycles.

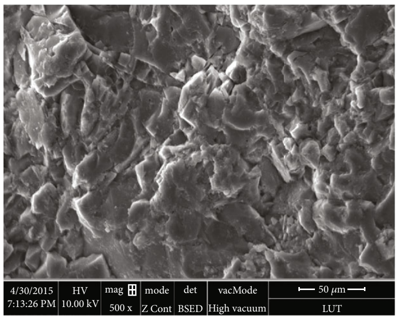

(a) Zero

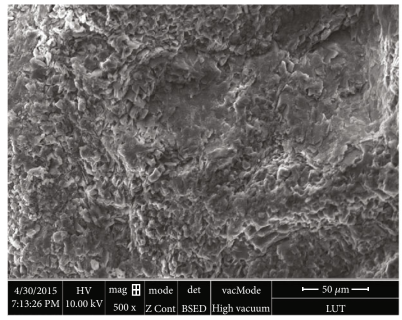

(b) 5 times

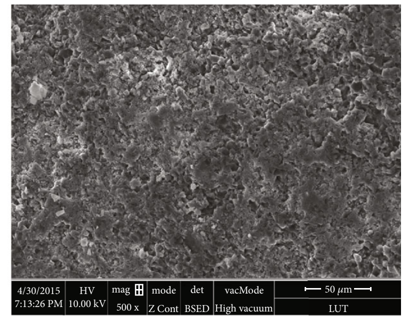

(c) 10 times

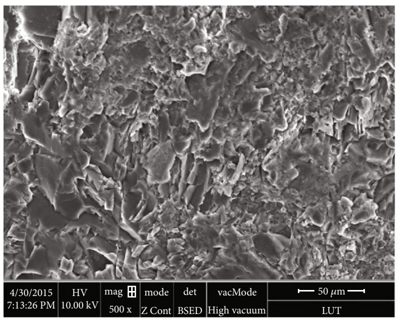

(d) 20 times

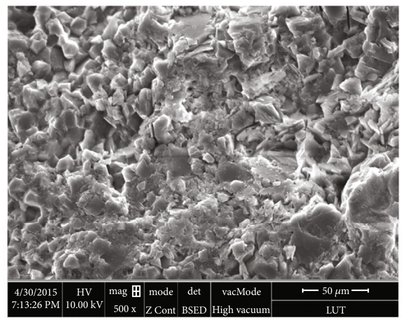

(e) 30 times

(a) SEM photographs of slate with increasing number of F-T cycles

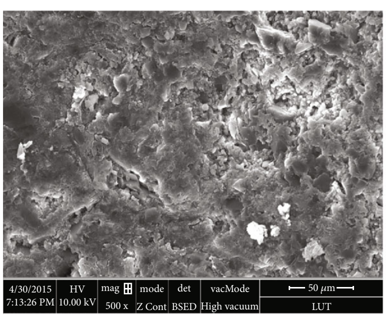

(a) Zero

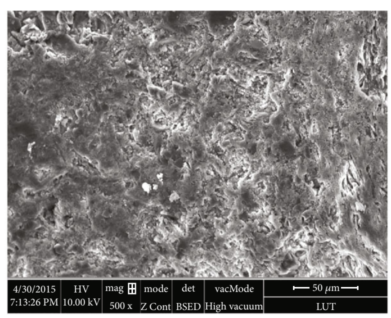

(b) 5 times

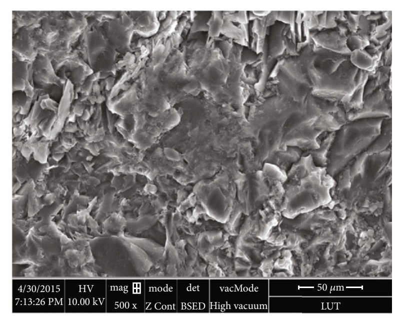

(c) 10 times

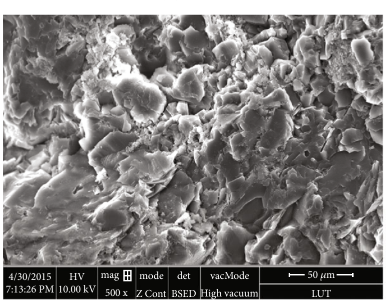

(d) 20 times

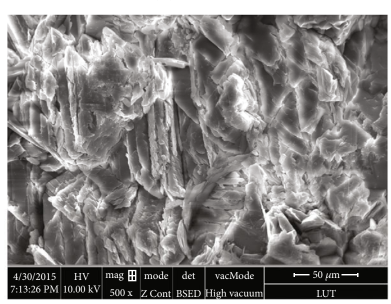

(e) 30 times

(b) SEM photographs of phyllite

Figure 11: SEM photographs of two low-grade metamorphic rocks.

low-grade metamorphic rocks that respond visibly to weathering techniques like freeze-thaw weathering. These processes may cause the rock to lose both its mechanical and physical qualities and fracture along its foliations.

Macrophotograph, quality test, macrophotograph wave velocity test, and uniaxial compression test were applied to study the processes in the two low-grade metamorphic rocks subjected to freeze-thaw cycles. These tests showed quality, wave velocity, and compressive strength decreased. According to the weathering index, wave velocity, stress-strain curve, and compressive strength, the various types of metamorphic rocks responded to freeze-thaw cycles in the following order: slate samples > phyllite samples.

XRD analyses were conducted to study the processes and mechanisms operating in low-grade metamorphic rock subjected to F-T cycles. These tests showed that the most

Table 2: SEM parameters of the low-grade metamorphic rock samples.

| Samples | Number of F-T cycles | Particle size ($\mu$m) | Porosity (%) | Pore width ($\mu$m) |
|---|---|---|---|---|
| Slate | 0 | 6-15 | 15-20 | 3-5 |
| | 5 | 10-20 | 18-25 | 6-8 |
| | 10 | 10-20 | 18-25 | 6-8 |
| | 20 | 15-20 | 20-30 | 6-8 |
| | 30 | 20-25 | 25-30 | 10-15 |
| Phyllite | 0 | 4-10 | 10-15 | 1-3 |
| | 5 | 6-10 | 12-20 | 2-6 |
| | 10 | 6-10 | 12-20 | 2-6 |
| | 20 | 8-15 | 15-25 | 5-10 |
| | 30 | 10-18 | 15-25 | 8-12 |

significant changes in mineral composition with weathering were the disappearance of feldspar, calcite, pyrite, and mica and a large increase in clay and gypsum contents. These changes in mineral composition were not controlled by the original composition of the material but were caused by weathering associated with F-T cycles, because the mica, feldspar, soda feldspar, and calcite are easily degraded during F-T cycles. In addition, feldspar is easily weathered under normal temperature and pressure conditions to produce illite or kaolinite.

The mica corrosion reactions are as follows:

$$\begin{aligned} &KAl_3Si_3O_{10}(OH)_2 + 6SiO_2 + 2K^+ \longrightarrow 3KAlSi_3O_8 + 2H^+ \\ &KAl_3Si_3O_{10}(OH)_2 + 6SiO_2 + 3Na^+ \longrightarrow 3NaAlSi_3O_8 + 2H^+ + K^+ \end{aligned} \tag{3}$$

The feldspar corrosion reactions are as follows:

$$\begin{aligned} &2KAl_3Si_3O_8 + 2H^+ + 9H_2O \longrightarrow Al_2Si_3O_8(OH)_4 + 2K^+ + 4H_4SiO_4 \\ &3KAlSi_3O_8 + 2H^+ + 12H_2O \longrightarrow KAl_3Si_3O_{10}(OH)_2 + H_4SiO_4 + 2K^+ \end{aligned} \tag{4}$$

The soda feldspar corrosion reactions are as follows:

$$2NaAlSi_3O_8 + 2H^+ + 9H_2O \longrightarrow Al_2Si_2O_5(OH)_4 + 2Na^+ + 4H_4SiO_4 \tag{5}$$

The calcite corrosion reactions are as follows:

$$CaCO_3 + 2H^+ \longrightarrow Ca^{2+} + H_2O + CO_2 \tag{6}$$

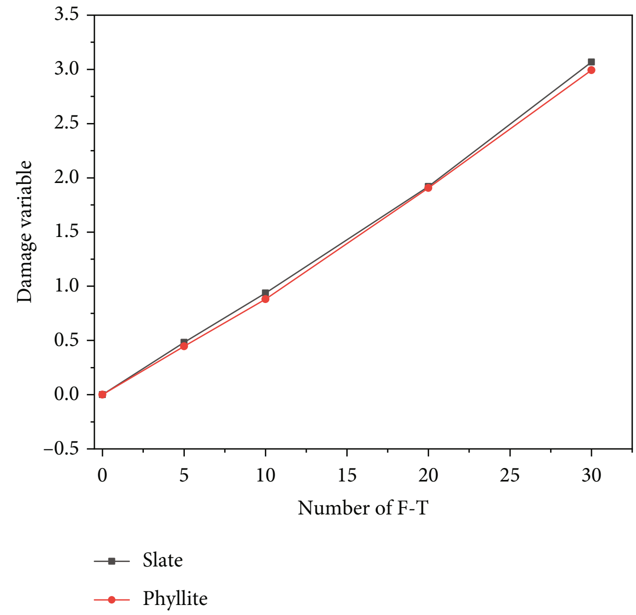


Figure 12: Damage variables of specimens under different hydrothermal conditions versus the number of cycles.

The pyrite corrosion reactions are as follows:

$$\begin{aligned} &FeS_2 + \frac{1}{2}O_2 + 2\,H^+ \longrightarrow Fe^{2+} + S_2 + H_2O \\ &FeS_2 + 3.5\,O_2 + H_2O \longrightarrow Fe^{2+}2SO_4^{2-} + 2H^+ \\ &2Fe^{2+} + \frac{1}{2}O_2 + 2H^+ \longrightarrow 2Fe^{3+} + H_2O \end{aligned} \tag{7}$$

*4.2. Damage Analysis.* The above SEM microstructure and mineral composition analysis of the specimens qualitatively revealed that the different degrees of changes in pore type, number, and connectivity of the specimens by different hydrothermal actions are the essential reasons for the different degrees and cumulative damage of the specimens. Therefore, the change in porosity was introduced as the basis for establishing the damage variable $D$ [38] to quantitatively evaluate the degree of specimen damage in specimens under different hydrothermal effects. This damage variable can quantitatively reflect the degree of internal microstructural damage in slate and micrite, and the relationship between the damage variable $D$ and pore space was calculated by the equation below. The damage variables are

$$\begin{aligned} &D = \frac{n_{(t1)} - n_{(t0)}}{1 - n_{(t0)}} = 1 - \frac{1 - n_{(t1)}}{1 - n_{(t0)}}, \\ &\frac{1}{v_{p(t)}} = \frac{1 - n_{(t)}}{v_m} + \frac{n_{(t)}}{v_f}, \\ &n_{(t)} = \frac{a}{v_{p(t)}} + b, \\ &a = \frac{v_m v_f}{v_m - v_f}, \\ &b = \frac{-v_f}{\left(v_m - v_f\right)}, \end{aligned} \tag{8}$$

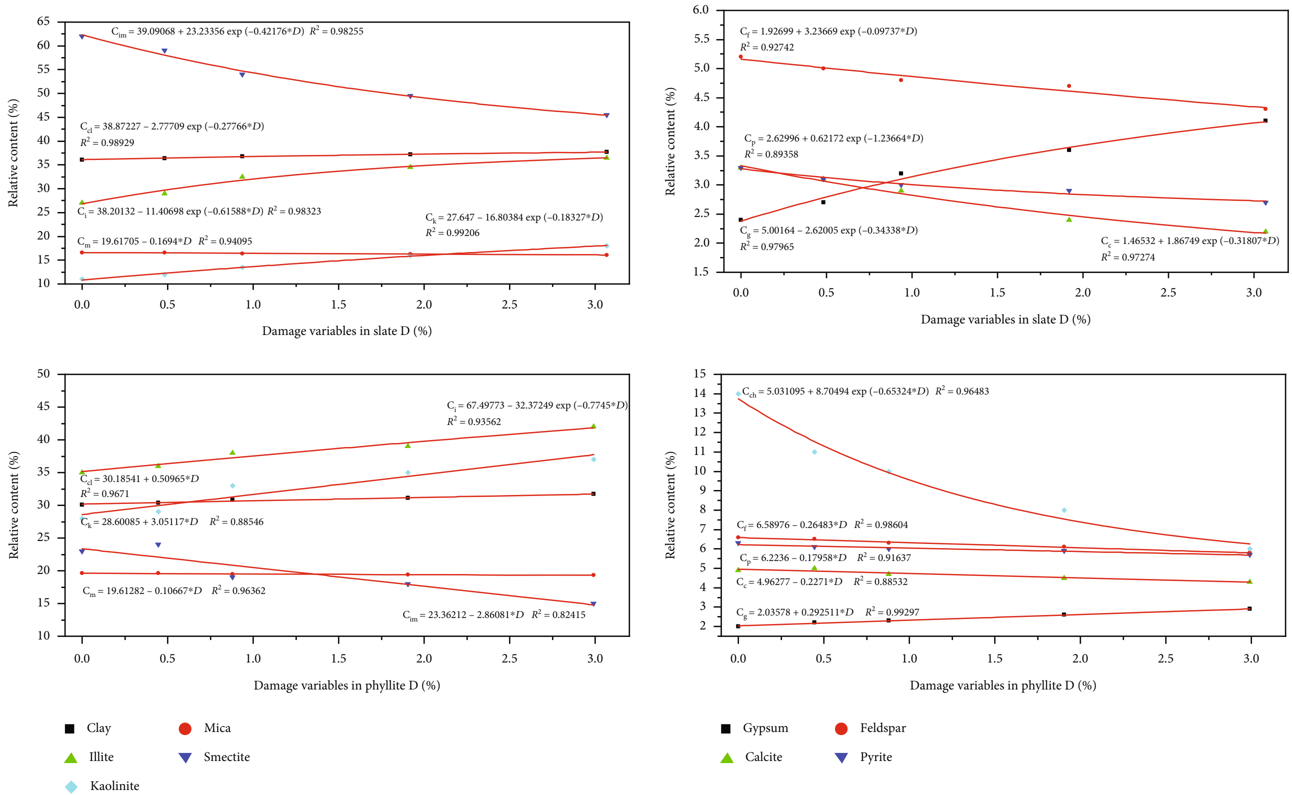


Figure 13: Relationship between mineral content of specimens and damage variables.

where $n_{(t0)}$ is the original void ratio of metamorphic sandstone, $n_{(t1)}$ is the void ratio after $t_1$ cycles of freeze-thaw, $v_{p(t)}$ is the measured longitudinal wave velocity (m/s) of the specimen after $t$ cycles, $v_m$ is the standard value of longitudinal wave velocity (m/s) of the metamorphic sandstone specimen, $v_m$ can be taken as the velocity of fresh sample from Section 3.3, $v_f$ is the fluid wave velocity (m/s) in the void, and $v_f$ can be taken as 1500 m/s in aqueous chemical solutions.

Since the lithology of this specimen is the same, $a$ and $b$ are constant, and the void ratio is only a function of the longitudinal wave velocity of the sandstone specimen at this time. From equation (8), the calculation result is $a = 2301$ and $b = -0.53$ for slate and $a = 2358$ and $b = -0.57$ for phyllite, where the values of $v_m$ and $v_f$ are selected from Section 3.2. The results of the damage variable $D$ are shown in Figure 12.

For purpose of clarifying the quantitative relationship between microstructural changes and mineral content of slate and micrite specimens, the fitted regression analysis was performed on the damage variable $D$ and its mineral composition of specimens under F-T effect (Figure 12), and the fitted equations and correlation coefficients were compiled (Figure 13).

The results showed that the correlation coefficients between the mineral content Ct and the damage variable $D$ of the specimens under F-T effects were all greater than 0.806. The correlation coefficients were greater than 0.893 for slate and 0.824 for phyllite rock, respectively, which demonstrated that the microstructural changes correspond with compound contents of the specimens quantitatively under F-T effect. The mineral contents of the specimens were analyzed freeze-thaw effects, and it was found that there were different correspondences between the mineral contents of the specimens and the damage variables. The clay minerals and gypsum were positively correlated with the damage variables; that is, the clay minerals and gypsum contents tended to increase with the microscopic damage, while pyrite, feldspar, calcite, and mica were negatively correlated with the damage variables. It shows that the content of these minerals decreases with the increase of microscopic damage. Meanwhile, the specimens were analyzed in depth for kaolinite and other clay minerals, and the results showed that kaolinite and illite were positively correlated with the damage variables, while smectite and chlorite were negatively correlated.

*4.3. Damage Mechanism.* The most remarkable changes in the low-grade metamorphic rocks of slate and phyllite were the increases in void space and water content. The corrosion of mica, feldspar, and calcite increased the void space, and the formation of channels increased the free water content. Furthermore, the clay minerals and gypsum adsorbed more water and increased the free water content. The volume of free water in the slate expanded during the freezing process and generated microcracks, and more water was absorbed during the thawing process. These processes and mechanisms were repeated sequentially to deteriorate the slate.

Liquid and solid phases can vary during F-T weathering. Free water that has been allowed to accumulate in the rock's pores freezes, enlarging the mineral particles and causing localized changes in the tension of the rock that stop volume expansion. This process changes the particle morphology and holes generated by corrosion of minerals such as feldspar, calcite, and mica, which are squeezed by stress to expand the void space. This results in structural alterations due to elastic-plastic deformation [39]. The migration of water vapour and tension release during thawing restore flexibility; however, any plastic deformation is retained. Meanwhile, the feldspar, calcite, and mica contents will decrease, and new voids will be generated, containing more water. The original and new clay minerals will absorb more water, further increasing the amount of free water. In conclusion, expanding pores and increasing clay mineral and gypsum contents increase the amount of free water available to the F-T process. This action is repeated over several F-T cycles; the plastic deformation piles up to produce a localized area of damage. As the region grows, the fundamental structure of the rock is gradually damaged, resulting in microfissures that spread further and reduce the overall strength of the rock.

## 5. Conclusions

The changes in macroscopic properties, and mechanical property in particular, on the deterioration of metamorphic rock such as slate and phyllite subjected to F-T test were investigated, and the influence of mineral content during above test was researched. The main conclusions can be summarised as follows:

(1) The weathering of metamorphic rock of slate and phyllite on the superficial slope under F-T weathering processes is an important replenishment for source material of debris flow. In addition, the investigation also finds the source material reserves at debris flow gully falling from the metamorphic rocks of slate and phyllite slope, 33.30% all source material

(2) The findings of studies on wave velocity and uniaxial compression show that freeze-thaw weathering processes clearly modify the macroscopic shape, quality, wave velocity, stress-strain curve, and compressive strength of slate and phyllite metamorphic rocks. Slate > phyllite were the two metamorphic rocks that underwent the greatest changes through weathering

(3) XRD analysis results for two kinds of metamorphic rocks both indicate corrosion of calcite, feldspar, and mica, and generation of gypsum and clay minerals after reiterant freeze-thaw cycles is the primary cause of metamorphic rocks of slate and phyllite deterioration. Furthermore, XRD analysis showed the clay mineral content and gypsum content increased with increasing numbers of F-T cycles; however, the feldspar, calcite, and mica contents decreased. Thus, these results indicate clear changes in mineral contents after repeated F-T cycles. The content of clay and gypsum followed the sequence of slate > phyllite, but the content of mica, feldspar, calcite, and pyrite followed the sequence of slate < phyllite

(4) The damage variable $D$ was established based on the change of void fraction of metamorphic sandstone, and it was concluded that the damage variable $D$ increased with the increase of the cycle number of metamorphic sandstone. With the increasing of damage variable, the mass change rate, longitudinal wave velocity, and peak intensity of metamorphic sandstone gradually decreased, among which the mass change rate was exponentially correlated with the damage variable, and the longitudinal wave velocity and peak intensity were negatively linearly correlated with the damage variable

## Data Availability

All data, models, and code generated or used during the study appear in the submitted article.

## Conflicts of Interest

The authors declare that they have no conflicts of interest.

## Acknowledgments

This study was supported by the National Natural Science Foundation of China (Grant No. 42107206), the Program for Changjiang Scholars and Innovative Research Team in University of the Ministry of Education of China (No. 2017IRT17051), the “Hongliu Excellent Young” Talents Support Program of Lanzhou University of Technology, and the National Natural Science Foundation of Gansu (Grant No. 22JR5RA292).

## References

[1] M. Van Den Eeckhaut and J. Hervás, “State of the art of national landslide databases in Europe and their potential for assessing landslide susceptibility, hazard and risk,” *Geomorphology*, vol. 139-140, pp. 545–558, 2012.

[2] N. P. Bhandary, R. Yatabe, R. K. Dahal, S. Hasegawa, and H. Inagaki, “Areal distribution of large-scale landslides along highway corridors in central Nepal,” *Georisk: Assessment and Management of Risk for Engineered Systems and Geohazards*, vol. 7, no. 1, pp. 1–20, 2013.

[3] M. B. Su, I. H. Chen, and C. H. Liao, “Using TDR cables and GPS for landslide monitoring in high mountain area,” *Journal of Geotechnical and Geoenvironmental Engineering*, vol. 135, no. 8, pp. 1113–1121, 2009.

[4] T. Zhu, J. Chen, D. Huang, Y. Luo, Y. Li, and L. Xu, “A DEM-based approach for modeling the damage of rock under freeze–thaw cycles,” *Rock Mechanics and Rock Engineering*, vol. 54, no. 6, pp. 2843–2858, 2021.

[5] C. Zhu, X. Xu, W. Liu et al., “Softening damage analysis of gypsum rock with water immersion time based on laboratory experiment,” *IEEE Access*, vol. 7, pp. 125575–125585, 2019.

[6] S. Huang, Y. Cai, Y. Liu, and G. Liu, “Experimental and theoretical study on frost deformation and damage of red

sandstones with different water contents," *Rock Mechanics and Rock Engineering*, vol. 54, no. 8, pp. 4163–4181, 2021.

[7] T. C. Chen, N. Mori, T. Suzuki, T. Shoji, and T. Goto, "Experimental study on crack development of rock specimens by freezing and thawing cycles," *Soils and Foundations*, vol. 40, no. 2, pp. 41–48, 2000.

[8] T. C. Chen, M. R. Yeung, and N. Mori, "Effect of water saturation on deterioration of welded tuff due to freeze-thaw action," *Cold Regions Science and Technology*, vol. 38, no. 2-3, pp. 127–136, 2004.

[9] G. G. Amoroso and V. Fassina, "Stone decay and conservation," in *Materials Science Monograph, Vol. II*, Elsevier, Amsterdam, 1983.

[10] Y. Lu, X. Chen, J. Tang et al., "Relationship between pore structure and mechanical properties of shale on supercritical carbon dioxide saturation," *Energy*, vol. 172, pp. 270–285, 2019.

[11] U. Kuila and M. Prasad, "Specific surface area and pore-size distribution in clays and shales," *Geophysical Prospecting*, vol. 61, no. 2, pp. 341–362, 2013.

[12] A. Jamshidi, M. R. Nikudel, and M. Khamehchiyan, "A novel physico-mechanical parameter for estimating the mechanical strength of travertines after a freeze–thaw test," *Bulletin of Engineering Geology and the Environment*, vol. 76, no. 1, pp. 181–190, 2017.

[13] S. Huang, S. Yu, Y. Ye, Z. Ye, and A. Cheng, "Pore structure change and physico-mechanical properties deterioration of sandstone suffering freeze-thaw actions," *Construction and Building Materials*, vol. 330, article 127200, 2022.

[14] Y. Wang, W. K. Feng, H. J. Wang, C. H. Li, and Z. Q. Hou, "Rock bridge fracturing characteristics in granite induced by freeze-thaw and uniaxial deformation revealed by AE monitoring and post-test CT scanning," *Cold Regions Science and Technology*, vol. 177, article 103115, 2020.

[15] S. Duca, C. Occhiena, and L. Sambuelli, "A procedure to determine the optimal sensor positions for locating AE sources in rock samples," *Rock Mechanics and Rock Engineering*, vol. 48, no. 2, pp. 481–493, 2015.

[16] T. Yamabe and K. M. Neaupane, "Determination of some thermo-mechanical properties of Sirahama sandstone under subzero temperature condition," *International Journal of Rock Mechanics and Mining Sciences*, vol. 38, no. 7, pp. 1029–1034, 2001.

[17] C. H. Sondergeld and C. S. Rai, "Velocity and resistivity changes during freeze-thaw cycles in Berea sandstone," *Geophysics*, vol. 72, no. 2, pp. E99–E105, 2007.

[18] J. Zhang, H. Deng, A. Taheri, B. Ke, and C. Liu, "Deterioration and strain energy development of sandstones under quasi-static and dynamic loading after freeze-thaw cycles," *Cold Regions Science and Technology*, vol. 160, pp. 252–264, 2019.

[19] Y. Liu, Y. Cai, S. Huang, Y. Guo, and G. Liu, "Effect of water saturation on uniaxial compressive strength and damage degree of clay-bearing sandstone under freeze-thaw," *Bulletin of Engineering Geology and the Environment*, vol. 79, no. 4, pp. 2021–2036, 2020.

[20] S. Huang, Y. He, X. Liu, and Z. Xin, "Experimental investigation of the influence of dry-wet, freeze-thaw and water immersion treatments on the mechanical strength of the clay-bearing green sandstone," *International Journal of Rock Mechanics and Mining Sciences*, vol. 138, article 104613, 2021.

[21] L. M. del Roa, F. Lopez, F. J. Esteban et al., "Ultrasonic study of alteration processes in granites caused by freezing and thawing," in *IEEE Ultrasonics Symposium, 2005*, pp. 415–418, Rotterdam, Netherlands, September 2005.

[22] H. Yavuz, "Effect of freeze–thaw and thermal shock weathering on the physical and mechanical properties of an andesite stone," *Bulletin of Engineering Geology and the Environment*, vol. 70, no. 2, pp. 187–192, 2011.

[23] L. M. del Río, F. López, F. J. Esteban et al., "Ultrasonic characterization of granites obtained from industrial quarries of Extremadura (Spain)," *Ultrasonics*, vol. 44, pp. e1057–e1061, 2006.

[24] X. Tan, W. Chen, J. Yang, and J. Cao, "Laboratory investigations on the mechanical properties degradation of granite under freeze–thaw cycles," *Cold Regions Science and Technology*, vol. 68, no. 3, pp. 130–138, 2011.

[25] F. Bayram, "Predicting mechanical strength loss of natural stones after freeze–thaw in cold regions," *Cold Regions Science and Technology*, vol. 83-84, pp. 98–102, 2012.

[26] J. Martínez-Martínez, D. Benavente, M. Gomez-Heras, L. Marco-Castaño, and M. Á. García-del-Cura, "Non-linear decay of building stones during freeze–thaw weathering processes," *Construction and Building Materials*, vol. 38, pp. 443–454, 2013.

[27] H. Mao and C.-H. Yang, "Study on effects of discontinuities on mechanical characters of slate," *Chinese Journal of Rock Mechanics and Engineering*, vol. 24, no. 20, pp. 3651–3656, 2005.

[28] H. Mao, C. Yang, X. Huang, and X. Wang, "Experimental study and theoretical analysis of slates under different saturated conditions," *Rock and Soil Mechanics*, vol. 9, no. 6, pp. 1637–1642, 2006.

[29] N. Sheng, M. C. Boyce, D. M. Parks, G. C. Rutledge, J. I. Abes, and R. E. Cohen, "Multiscale micromechanical modeling of polymer/clay nanocomposites and the effective clay particle," *Polymer*, vol. 45, no. 2, pp. 487–506, 2004.

[30] K. Cui, G. Wu, X. Wang, W. Chen, and H. Liu, "Drying-wetting-saturating experiments for deterioration of physical and mechanical properties of slate," *Journal of Engineering Geology*, vol. 23, no. 6, pp. 1045–1052, 2015.

[31] K. Cui, G. Wu, X. Wang, and W. Chen, "Behaviour of slate following freeze–thaw and dry–wet weathering processes," *Quarterly Journal of Engineering Geology and Hydrogeology*, vol. 50, no. 2, pp. 117–125, 2017.

[32] K. Cui, G. Wu, X. Wang, W. Chen, and H. Liu, "Research on the behavior and mechanism of the slate from the slope at the gully of debris flow respond to climate environment," *Chinese Journal of Rock Mechanics and Engineering*, vol. 35, Supplement 1, pp. 360–368, 2016.

[33] B. Yuan, Z. Li, Y. Chen et al., "Mechanical and microstructural properties of recycling granite residual soil reinforced with glass fiber and liquid-modified polyvinyl alcohol polymer," *Chemosphere*, vol. 268, article 131652, 2022.

[34] B. Yuan, Z. Li, W. Chen et al., "Influence of groundwater depth on pile–soil mechanical properties and fractal characteristics under cyclic loading," *Fractal and Fractional*, vol. 6, no. 4, p. 198, 2022.

[35] B. Yuan, M. Chen, W. Chen, Q. Luo, and H. Li, "Effect of pile-soil relative stiffness on deformation characteristics of the laterally loaded pile," *Advances in Materials Science and Engineering*, vol. 2022, Article ID 4913887, 13 pages, 2022.

[36] B. Yuan, W. Chen, J. Zhao, F. Yang, Q. Luo, and T. Chen, "The effect of organic and inorganic modifiers on the physical properties of granite residual soil," *Advances in Materials Science and Engineering*, vol. 2022, Article ID 9542258, 13 pages, 2022.

[37] B. Yuan, Z. Li, Z. Zhao, H. Ni, Z. Su, and Z. Li, "Experimental study of displacement field of layered soils surrounding laterally loaded pile based on transparent soil," *Journal of Soils and Sediments*, vol. 21, no. 9, pp. 3072–3083, 2021.

[38] W. Ding and X. Feng, "Study on chemical damage effect andquantitative analysis method of meso-structure of limestone," *Chinese Journal of Rock Mechanics and Engineering*, vol. 24, no. 8, pp. 1283–1288, 2005.

[39] D. T. Nicholson and F. H. Nicholson, "Physical deterioration of sedimentary rocks subjected to experimental freeze-thaw weathering," *Earth Surface Processes and Landforms*, vol. 25, no. 12, pp. 1295–1307, 2000.